Journal of Electromagnetic Waves and Applications, 2013
Vol. 27, No. 9, 1100–1113, http://dx.doi.org/10.1080/09205071.2013.801040

A comparison of NSGA-II, DEMO, and EM-MOPSO for the multi-objective design of concentric rings antenna arrays

Marco A. Panduro[a]*, Carlos A. Brizuela[b], Jesus Garza[a], Sergio Hinojosa[a] and Alberto Reyna[a]

[a]*Unidad Académica Multidisciplinaria Reynosa-Rodhe, Universidad Autónoma de Tamaulipas (UAT), Carretera Reynosa-San Fernando, Reynosa, Tamaulipas 88779, México;* [b]*CICESE Research Center Carretera Ensenada-Tijuana 3918, Ensenada Baja, California 22860, México*

(*Received 2 January 2013; accepted 28 April 2013*)

A comparison between different modern multi-objective optimization methods applied to the design of concentric rings antenna arrays is presented in this paper. This design of concentric rings antenna arrays considers the optimization of the amplitude and phase excitations across the antenna elements in order to generate the trade-off curves between side lobe level and directivity for a scannable pattern with optimal performance in the whole azimuth plane. Simulation results by using evolutionary multi-objective optimization methods, such as: NSGA-II, DEMO, and EM-MOPSO are provided in this document. Furthermore, a comparative analysis of the performance between these algorithms is presented.

1. Introduction

Recently, multi-objective evolutionary algorithms have been applied to several antenna arrays design problems.[1,2] The most representative multi-objective algorithms include the NSGA-II,[3–4] DEMO,[5] and MOPSO,[6] among others. Since antenna arrays design is a complex task involving multiple objectives, these techniques have received great attention because they can solve a variety of problems and are easy to implement.

This paper presents a comparison of NSGA-II, DEMO, and EM-MOPSO for the multi-objective design of concentric rings antenna arrays. The purpose and contribution of this paper is to present a comparative evaluation of NSGA-II, DEMO, and EM-MOPSO in their performances to design concentric rings antenna arrays. The multi-objective design of concentric rings antenna arrays considers the optimization of the amplitude and phase excitations across the antenna elements in order to generate the trade-off curves between the side lobe level and directivity for a scannable pattern with optimal performance in the whole azimuth plane, i.e., in a scanning range of $[0°, 360°]$.

To the best of the authors knowledge, a performance comparison of NSGA-II, DEMO, and EM-MOPSO applied to the design of concentric rings antenna arrays (with a scannable pattern) has not been presented previously.

The remainder of the paper is organized as follows. Section II states the antenna array design problem we are dealing with. Section III describes the evolutionary multi-objective optimization algorithms employed. Section IV presents and discusses

*Corresponding author. Email: mamendoza@uat.edu.mx

the simulation results. Finally, the summary and conclusions of this work are presented in Section V.

2. Problem statement

Consider a concentric rings array of N_T elements are uniformly spaced on the *x–y* plane as shown in Figure 1. The array factor for this concentric ring array shown in Figure 1 is given by Balanis [7]

$$AF(\theta, \varphi, W) = \sum_{n=1}^{N_r} \sum_{m=1}^{N_n} w_{nm} \exp\{jkr_n[u \cos \varphi_m + v \sin \varphi_m]\} \tag{1}$$

In this case, the previous array factor for concentric rings array with phase excitation is formulated by incorporating the element phase perturbation P as follows:

$$AF(\theta, \varphi, W, P) = \sum_{n=1}^{N_r} \sum_{m=1}^{N_n} w_{nm} \exp\{j[kr_n(u \cos \varphi_m + v \sin \varphi_m) + \delta_{nm}]\} \tag{2}$$

where

$$u = \sin\theta \cos\varphi - \sin\theta_0 \cos\varphi_0 \tag{3}$$

$$v = \sin\theta \sin\varphi - \sin\theta_0 \sin\varphi_0 \tag{4}$$

N_r represents the number of rings; N_n represents the number of elements on the ring n; r_n is the radius of ring n; λ is the signal wavelength; $k = 2\pi/\lambda$ is the phase constant; $\varphi_m = 2\pi(m-1)/N_n$ represents the angular position of the element m on the ring n; (θ_0, φ_0) is the direction of the maximum radiation; θ is the angle of a plane wave in the elevation plane; φ is the angle of a plane wave in the azimuth plane; w_{nm} and δ_{nm} are

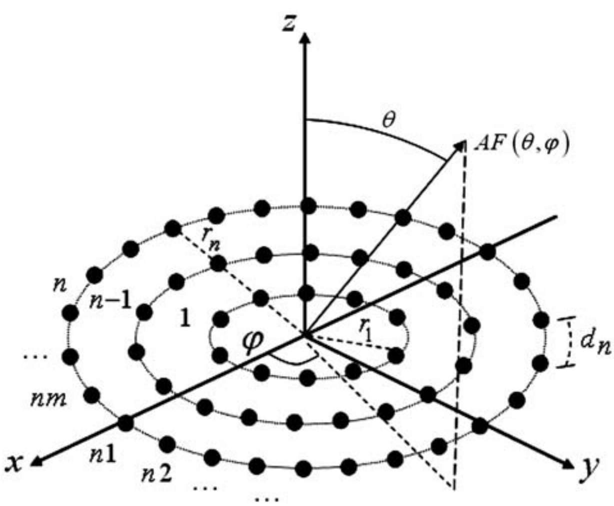

Figure 1. Steerable concentric rings array with antenna elements uniformly spaced.

the amplitude excitations and phase perturbations of the element m on the ring n defined by the sets W and P. In these sets, the amplitude excitations and phase perturbations for the entire rings are arranged in two vectors of real numbers as follows:

$$W = [w_{11}, w_{12}, \ldots, w_{1N_1}, w_{21}, w_{22}, \ldots, w_{2N_2}, \ldots, w_{n1}, w_{n2}, \ldots, w_{nN_n}] \quad (5)$$

$$P = [\delta_{11}, \delta_{12}, \ldots, \delta_{1N_1}, \delta_{21}, \delta_{22}, \ldots, \delta_{2N_2}, \ldots, \delta_{n1}, \delta_{n2}, \ldots, \delta_{nN_n}] \quad (6)$$

The sets W and P are divided into subsets for each ring on the plane. Thus, there exist N_r subsets for amplitude excitations and N_r subsets for phase excitations. This model considers the center of each ring as the phase reference in the array factor. Furthermore, it is considered a symmetrical excitation for the rings and the behavior of the array factor in the azimuth plane ($0° \leqslant \varphi_0 \leqslant 360°$) with an angular step of 60° in the cut of $\theta = 90°$.

In order to include the effect of mutual coupling for the concentric rings array, the method of induced electro-motive force (EMF) [7] for thin and finite dipoles is considered. In this case, it is considered the side-by-side configuration and dipole lengths of $l = \lambda/2$.

Since N_n must be an even number, so that the symmetry could be correctly applied, the subset of amplitude excitations for the ring n is given as W_{n1}, W_{n2}, …, $W_{nNn/2}$, $W_{n(Nn/2)+1} = W_{n1}$, $W_{nNn} = W_{nNn/2}$. And the subset of phase excitations for the ring n is given as δ_{n1}, δ_{n2}, …, $\delta_{nNn/2}$, $\delta_{n(Nn/2)+1} = -\delta_{n1}$, …, $\delta_{nNn} = -\delta_{nNn/2}$. The amplitude and phase excitations in the subsets of the entire ring could be rotated on antenna element position for beam steering.

To illustrate this, it could be considered an array of just one ring of m elements, i.e., a circular array. If we select the number of antenna elements as $N = 6$ (as an example) and there is a constant angular separation of 60° between different beam steering angles, the optimal excitation for a particular beam steering angle should also apply to other beam steering angles by simply substituting (W_m, δ_m) into (W_{m+1}, δ_{m+1}) when the beam steering angle is increased by 60°.[8]

The rotation properties could be similarly applied to the entire rings as mentioned in the case of one ring. In this design case, we consider a concentric rings array with N_r rings. The main lobe is steered with an angular step of 60° in azimuth plane. Because of that, the number of elements for the rings is given in other way $N_1 = 360°/60°$, $N_2 = 2N_1$, …, $N_n = nN_1$ elements. In order to keep a uniform element distribution, the radius of the rings are r_1, $r_2 = 2r_1$, $r_3 = 3r_1$, …, $r_n = nr_1$ and the spacing element is set as $d_n = 2\pi N_n r_n$. Note that the antenna elements distribution does not consider a central element on the origin.

In this case, the optimal sets of amplitude and phase excitations for a certain direction of the beam steering φ_0 should also apply to other direction of beam steering ($\varphi_0 + 60°$) by rotating the subsets of amplitude and phase excitations of the rings of the array. Hence, the excitations (W_{nm}, δ_{nm}) for the element m of ring n are now substituted into the positions ($W_{n(m+n)}$, $\delta_{n(m+n)}$) in the subsets of amplitude and phase excitations of the ring n for each steering direction.

By means of this design, only one optimization is required for beam steering in steps of 60° degrees rather than one optimization for each beam steering direction.

The objective functions of this design problem can be formulated as follows:

$f_1 = SLL_{\max}(W, P)$ and $f_2 = 1/DIR(W, P)$.

where SLL_{max} is the maximum side lobe level attained in $\varphi = [-\pi, \pi]$ and DIR represents the directivity of the array factor. Thus, the optimization task is then in the first component: the minimization of the maximum side lobe level (f_1), and in the second component it is the maximization of the directivity (f_2). Then the problem can be formulated as:

$$\text{Minimize } (f_1, f_2) \tag{7}$$

$$\text{subject to}(P \in M),\ (W \in \Lambda),$$

where $M = (0,\ 2\pi]^N$ and $\Lambda = [W_{min},\ W_{max}]^N$ is thez range of the weight coefficients imposed for practical implementation of the attenuators. Notice that the relations between the decision variables P and W with f_1, f_2 are not trivial, but highly nonlinear.

Please note that, once the corresponding array factor has been computed for one desired direction i.e. $\varphi_0 = 0°$, the array factor could be scanned in steps of 60° in the azimuth plane ($0° \leqslant \varphi_0 \leqslant 360°$) by rotating the phase and amplitude excitations. As an advantage of the geometry of concentric rings for antenna arrays, the optimal properties of the side lobe level and the directivity are remained in each scanning direction by applying the rotation principle mentioned previously.

2.1. Previous work

In the application of multi-objective evolutionary optimization techniques for designing antenna arrays, the design of different array structures has been considered. Among these array structures, the linear and circular array has been studied in the works presented in [1] and [3,4]. In these works, in order to determine the trade-off curves of the side lobe level and main beam width for linear and circular antenna arrays the application of NSGA-II is illustrated.

An interesting open problem is to determine the trade-off curves for other array configurations, as in the case of concentric rings antenna arrays. In this case, array configurations, in which the elements are placed, in concentric rings are of great interest. They have applications in radio direction finding, air and space navigation, radar, and other systems.[9–13]

In the study of concentric rings antenna arrays, optimizing an array to have low side lobe level at broadside has been considered.[14–16] The design of a concentric ring antenna array in order to have a scannable pattern is dealt with in [2] and [17–19]. However, the application of evolutionary multi-objective techniques to design concentric rings antenna arrays has been rather scarce, a few related results can be found in the literature.[2] Moreover, a performance comparison of NSGA-II, DEMO, and EM-MOPSO applied to design concentric rings antenna arrays (with a scannable pattern) has not been presented previously.

The main contribution of this paper is the computation of the trade-off curves between the side lobe level and the directivity for concentric rings antenna arrays when the scanning of the array factor is considered. The elements of novelty presented in this paper are the application and comparison of different multi-objective evolutionary optimization algorithms to a design problem which is both nontrivial and interesting:

the multi-objective design of concentric rings antenna arrays with a scannable array factor. In this case, the term multi-objective is employed to illustrate the design that evaluates the performance criteria and at the same time in order to obtain the trade-off curve that represents the best compromise among the objectives.

Moreover, a performance comparison of NSGA-II, DEMO, and EM-MOPSO applied to design concentric rings antenna arrays (with a scannable pattern) has not been presented previously. Even more studies comparing the performance of different optimizers for antenna design have been scarce.[8]

The next section presents the multi-objective evolutionary optimization algorithms to be evaluated when they are applied to this design problem.

3. The multi-objective evolutionary optimization algorithms

As already being pointed out, the objective of this paper is to present a comparative evaluation of NSGA-II, DEMO, and EM-MOPSO for the design of concentric rings antenna arrays. Therefore, the main characteristics and the procedure for each algorithm are described in the next subsections.

3.1. The NSGA II

Genetic algorithms are especially well suited for multi-objective problems, since they are designed to handle a multi-set of solutions in a single iteration. We chose this algorithm proposed by Deb [20] for its easiness of implementation and its efficient computation of non-dominated ranks. The procedure for NSGA-II is described as follows.

Algorithm 1. NSGA-II.

Step 1. Set $r=0$. Generate an initial population $P[r]$ of *popSize* individuals.
Step 2. Classify the individuals according to a non-dominated ranking system.
Step 3. Set $i=1$.
Step 4. Use Binary Crowded Tournament Selection, apply crossover with probability *pc* and mutation with probability *pm*.
Step 5. Set $i=i+1$. If $i>popSize$ then go to Step 6 otherwise go to Step 4.
Step 6. REPLACEMENT. Assign ranks to individuals in the population generated by the union of Parents and Children populations. Copy into the new population individuals from a front with lower index as long as the number of individuals in the front does not overflow the population size (*popSize*). In the last front to be copied sort the individuals according to their crowding distance eliminating those individuals with smaller crowing distance, until the total number of individuals (*popSize*) is completed.
Step 7. Set $r=r+1$. If $r=rmax$ then STOP; otherwise go to STEP 3.

The main idea in STEP 2 is to classify the individuals according to their dominance relation, i.e. the set of non-dominated individuals are said to be in front 0. After removing these individuals the remained nondominated solutions are in front 1. The procedure continues until all individuals are assigned to a front. Deb [20] explains the procedures involved at each step of this algorithm in detail. The individual representations as well as the crossover and mutation operators are explained in the following subsections.

3.1.1. Individual representation and decoding

Each individual is, in general, represented by two vectors of real numbers (amplitude excitations and phase perturbations of the antenna elements). The individuals are encoded as a vector of real numbers, that represents the amplitudes, and as a vector of real numbers restrained to be on the range (0, 2π), that represents the phase perturbations of the antenna elements.

3.1.2. Genetic operators

The applied genetic operators are standard, the well-known two-point crossover [21] along with a single mutation where a locus is randomly selected and the allele is replaced by a random number uniformly distributed in the projection of the feasible region on the corresponding variable.

3.2. DEMO

It is a way of extending Differential Evolution (DE) [22] to be suitable for solving multi-objective optimization problems. The DEMO implementation differs from others and represents a novel approach to multi-objective optimization. DEMO can be implemented in three variants (DEMO/parent, DEMO/closest/dec, and DEMO/closest/obj).[5]

Algorithm 2. DEMO/parent.

Step 1. Evaluate the initial population P of random individuals.
Step 2. While the stopping criterion is not met, do:
- 2.1. For each individual Pi ($i = 1, \dots, popSize$) from P repeat:
  - (a) Create a candidate C from parent Pi.
  - (b) Evaluate the candidate.
  - (c) If the candidate dominates the parent, the candidate replaces the parent.
    If the parent dominates the candidate, the candidate is discarded.
    Otherwise, the candidate is added to the population.
- 2.2. If the population has more than *popSize* individuals, truncate it.
- 2.3. Randomly enumerate the individuals in P.

The main idea in STEP 2 is: the candidate replaces the parent if it dominates it. If the parent dominates the candidate, the candidate is discarded. Otherwise (when the candidate and parent are non-dominated with regard to each other), the candidate is added to the population. This step is repeated until *popSize* number of candidates are created. After that, we get a population of the size between *popSize* and $2 \times popSize$. If the population has enlarged, we have to truncate it to prepare it for the next step of the algorithm. The truncation consists of sorting the individuals with non-dominated sorting and then evaluating the individuals of the same front with the crowding distance metric. The truncation procedure keeps in the population only the best *popSize* individuals (with regard to these two metrics). The described truncation is derived from NSGA-II. For more details of this algorithm see [5].

The described DEMO's procedure outlined in this section is the most elementary of the three variants: DEMO/parent. The other two variants were inspired by the concept of Crowding DE.[23] Usually, the candidate is compared to its parent. In Crowding

DE, the candidate is compared to the most similar individual in the population. The applied similarity measure is the Euclidean distance between two solutions.

3.3. EM-MOPSO

This approach is based on Particle Swarm Optimization (PSO) [24] and uses Pareto dominance criteria for selecting non-dominated solutions; an external repository (*ERP*) for storing the best solutions found (elitism); crowding distance operator for creating effective selection pressure among the swarm to reach true Pareto optimal fronts; and incorporates an effective elitist-mutation (EM) strategy for effective exploration of the search space. The proposed elitist-mutated multi-objective PSO (EM-MOPSO) [25] algorithm is discussed in the following sections. More details of this algorithm can be found in [25].

Algorithm 3. EM-MOPSO.

Step 1. Initialize population. Set iteration counter $t=0$.
1. The current position of the *i*-th particle *Xi* is initialized with random real numbers within the established decision variable range; each particle velocity vector *Vi* is initialized with a uniformly distributed random number in [0,1].
2. Evaluate each particle in the population. The personal best position *Pi* is set to *Xi*.

Step 2. Identify particles that give non-dominated solutions in the current population and store them in an *ERP*.

Step 3. $t=t+1$.

Step 4. Repeat the loop (step through PSO operators):
1. Select randomly a global best *gbest* for the *i*-th particle from the *ERP*.
2. Calculate the new velocity *Vi* based on Equation (8), and the new *Xi* by Equation (9).

$$v_{id} = wv_{id} + c_1 r_1 (pbest_{i,d} - x_{id}) + c_2 r_2 (gbest_d - x_{id}), \quad v_i \leqslant v_{d,\max} \quad \forall d \tag{8}$$

$$x_{id} = x_{id} + v_{id} \Delta t \tag{9}$$

where each particle $X_i = (x_{i1}, \ldots, x_{iD})$ represents a potential solution (amplitude excitations and phase perturbations of the antenna elements) defined as a point in a D-dimensional space. The limits of the parameters x_{id} to be optimized, define the search space in D-dimensions. Iteratively, each particle i within the swarm flies over the solution space to a new position X_i with a velocity $V_i = (v_{i1},\ldots,v_{iD})$, both updated along each dimension d; w is known as the inertial weight, c_1 and c_2 are the acceleration constants and determine how much the particle is influenced by its best location (usually referred to as memory, nostalgia, or self-knowledge) and by the best position ever found by the swarm (often called shared information, cooperation, or social knowledge), respectively. Moreover, r_1 and r_2 represent two separate calls to a random number function U [0, 1], $v_{d,\max}$ is the maximum allowed velocity for each particle used as a constraint to control the exploration ability of the swarm and usually set to the

dynamic range of each dimension,[26] and Δt is a time-step usually chosen to be 1.0. The detailed interpretations of these step terms may be found in [26].
3. Repeat the loop for all the particles.

Step 5. Evaluate each particle in the population.
Step 6. Perform the Pareto dominance check for all the particles: if the current local best *Pi* is dominated by the new solution, then *Pi* is replaced by the new solution.
Step 7. Set *ERP* to a temporary repository, *TempERP* and empty *ERP*.
Step 8. Identify particles that give non-dominated solutions in the current iteration and add them to *TempERP*.
Step 9. Find the non-dominated solutions in *TempERP* and store them in *ERP*. The size of *ERP* is restricted to the desired set of non-dominated solutions; if it exceeds, use the crowding distance operator to select the desired ones. Empty the *TempERP*.
Step 10. Perform EM operation on established number of particles.
Step 11. Check for termination criterion; if it is not satisfied, then go to step 3; otherwise output the non-dominated solution set from *ERP*.

The main operators used in this algorithm are explained below.

3.3.1. Variable size ERP

The global best guide of the particles is selected from a restricted variable size *ERP*. This restriction on *ERP* is done using the crowding distance operator. This operator ensures that those non-dominated solutions with the highest crowding distance values are always preferred to be in the *ERP*. For effective exploration in the objective functions space, the size is initially set to 10% of maximum *ERP*, then the value is increased in a stepwise manner, so that at the start of 90% of maximum iterations, it reaches the maximum size of *ERP*. Selecting different guides for each particle from a restricted repository allows the particles to better explore the true Pareto optimal region. More details can be found in [25].

The results of using these evolutionary multi-objective optimization algorithms for the design of concentric rings antenna arrays are described in the next section.

4. Experimental setup and results

The methods of NSGA-II, DEMO, and EM-PSO were implemented to study the behavior of the array factor in the azimuth plane ($0° \leqslant \varphi_0 \leqslant 360°$) with an angular step of 60° in the cut of $\theta = 90°$. As mentioned before, the steerable concentric rings array considers a uniform distribution on a plane. To achieve so, it is proposed, $N_T = 90$ elements are distributed in $N_r = 5$ rings. Thus, the elements distribution is $N_1 = 6$, $N_2 = 12$, $N_3 = 18$, $N_4 = 24$, and $N_5 = 30$ for the array. Furthermore, the radius for the ring $n = 1$ is defined as $r_1 = 0.5\lambda$. For this configuration, the element spacing is $d_n \geq 0.5\lambda$. We give all algorithms the same computation time with equal computational resources.

In the case of EM-MOPSO we have set $c_1 = c_2 = 2.0$ as suggested by Eberhart and Shi [27] and Jin and Rahmat-Samii [28] for the sake of convergence. To further accelerate the convergence, a time-varying inertial weight, w, is utilized and varied from 0.9 at the beginning to 0.4 toward the end of the optimization.[29] The value of $v_{d,\max}$ in (8)

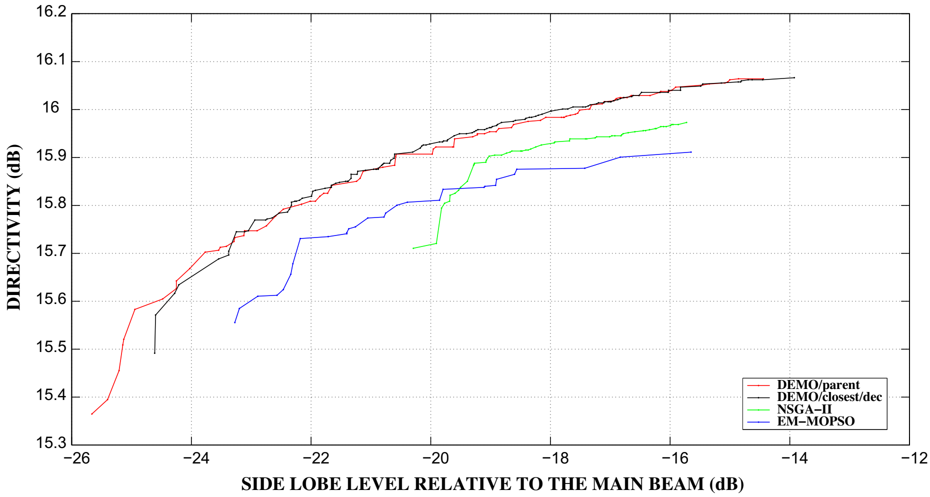

Figure 2. Trade-off curves between the side lobe level and the directivity for the concentric rings antenna array obtained by NSGA-II, EM-MOPSO, DEMO/parent and DEMO/closest/dec.

Table 1. Average time for the 30 runs of each algorithm and the number of iterations employed.

Average time (minutes)	Algorithm	Number of iterations
64.99	DEMO/closest/dec	250
65.8	DEMO/parent	400
65.34	NSGA-II	400
64.99	EM-MOPSO	700

Table 2. Set coverage C(A,B) between each pair of algorithms.

A	B	Set coverage
DEMO/parent	DEMO/closest/dec	0.25
DEMO/parent	NSGA-II	1
DEMO/parent	EM-MOPSO	1
DEMO/closest/dec	DEMO/parent	0.6383
DEMO/closest/dec	NSGA-II	1
DEMO/closest/dec	EM-MOPSO	1
NSGA-II	DEMO/parent	0
NSGA-II	DEMO/closest/dec	0
NSGA-II	EM-MOPSO	0.976
EM-MOPSO	DEMO/parent	0
EM-MOPSO	DEMO/closest/dec	0
EM-MOPSO	NSGA-II	0.0441

is set to $0.9r$ where r is the difference between the maximum and minimum values, each decision variable can achieve. For the case of NSGA-II, we have set the proposed parameters based mainly on our previous experience in solving similar problems.[1,3]. Two-point crossover along with standard single point mutation were used. In the DEMO algorithms the value of F is set to 0.5. The stopping criterion in each algorithm is the number of iterations. In order to have similar computation time, the number of iterations was set as follows: 400 for NSGA-II, 400 for DEMO/parent, 250 for DEMO/closest/dec, and 700 for EM-MOPSO. The population size for each algorithm is set to 500. Each algorithm was executed 30 times and the consolidated front for each run is considered.

Figure 2 shows the trade-off curves between the side lobe level and the directivity for the concentric rings antenna array obtained by NSGA-II, EM-MOPSO, DEMO/parent, and DEMO/closest/dec. The results shown in Figure 2 illustrate that the DEMO/parent and the DEMO/closest/dec algorithms found better non-dominated solutions as an approximation to the Pareto solution. The average time for the 30 runs of each algorithm and the number of iterations employed in each run are illustrated in Table 1. As it can be seen in Table 1 similar computation time was provided for each algorithm.

Table 2 shows the Set Coverage [30] between each pair of algorithms. As it can be seen in this table, DEMO/parent and DEMO/closest/dec covered totally to NSGA-II and to EM-MOPSO. Considering the Set Coverage between DEMO/parent and DEMO/closest/dec, it is observed that 64% of the solutions of DEMO/closest/dec covered to DEMO/parent. In this pair of algorithms, 25% of the solutions of DEMO/parent covered to DEMO/closest/dec. From this, DEMO/closest/dec presented a better perfor-

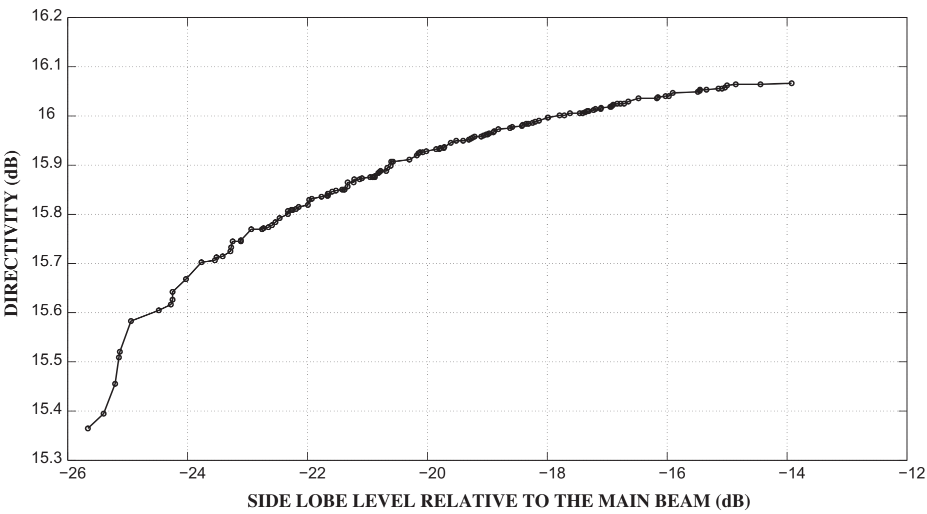

Figure 3. Non-dominated front of the best solutions obtained by each algorithm that are considered as the Pareto front in the calculus of the binary epsilon indicator.

Table 3. Value of the unary epsilon indicator for each algorithm.

PARETO FRONT (Figure 3)	DEMO/parent	1
PARETO FRONT (Figure 3)	DEMO/closest/dec	1
PARETO FRONT (Figure 3)	NSGAII	0.9873
PARETO FRONT (Figure 3)	EM-MOPSO	0.9615
DEMO/parent	PARETO FRONT (Figure 3)	1.0053
DEMO/closest/dec	PARETO FRONT (Figure 3)	1.1286
NSGAII	PARETO FRONT (Figure 3)	1.856
EM-MOPSO	PARETO FRONT (Figure 3)	1.5566

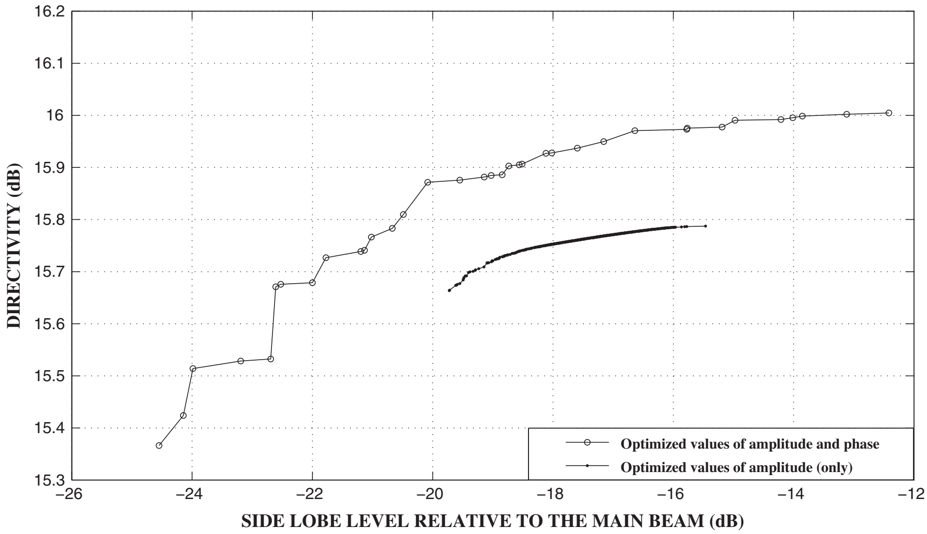

Figure 4. Trade-off curves between the side lobe level and the directivity for the concentric rings antenna array for optimized values of amplitude (only) and for optimized values of amplitude and phase (simultaneously).

mance with respect to DEMO/parent, NSGA-II, and EM-MOPSO for this performance metric.

Another metric to evaluate the relative performance of an evolutionary multi-objective optimization algorithm is the binary epsilon indicator.[30] This indicator takes two nondominated fronts as input and gives a measure of how much one of them needs to be improved, in order to dominate the other, i.e. it tells us how much two fronts are separated from each other. In this design problem, the set of Pareto solutions is not known. Therefore, to calculate the binary epsilon indicator and in order to make a fair comparison among the algorithms, the “best of the best” of all algorithms is obtained and considered as the Pareto front for the calculation of this metric, i.e. the nondominated front of the best solutions obtained by each algorithm after 30 runs was taken as representative front for that algorithm. Figure 3 shows the non-dominated front of the best solutions obtained by each algorithm. This figure shows a wide range of solutions between the directivity and the side lobe level for the design of concentric rings antenna arrays. The value of the binary epsilon indicator for each algorithm is illustrated in Table 3. This Table shows a better behavior on this metric for DEMO/parent and DEMO/closest/dec. However, DEMO/parent presented a better approximation to the Pareto front with respect to DEMO/closest/dec, NSGA-II, and EM-MOPSO.

As an interesting aspect, it included an example for computation of optimized values of amplitude (only) and for optimized values of amplitude and phase (simultaneously). In this case, the method of DEMO/parent was used in order to determine the optimized values for each case. The value of F is set to 0.5, the population size is set to 500, and the number of iterations is set to 1000. Figure 4 shows the trade-off curves between the side lobe level and the directivity for the concentric rings antenna array for each case. As it can be shown, the trade-off between the side lobe level and the directivity is better explained by optimizing the amplitude and phase (simultaneously) with respect to the amplitude only case. From a design point of view, a concentric rings antenna array with the amplitude and phase optimized simultaneously could provide a

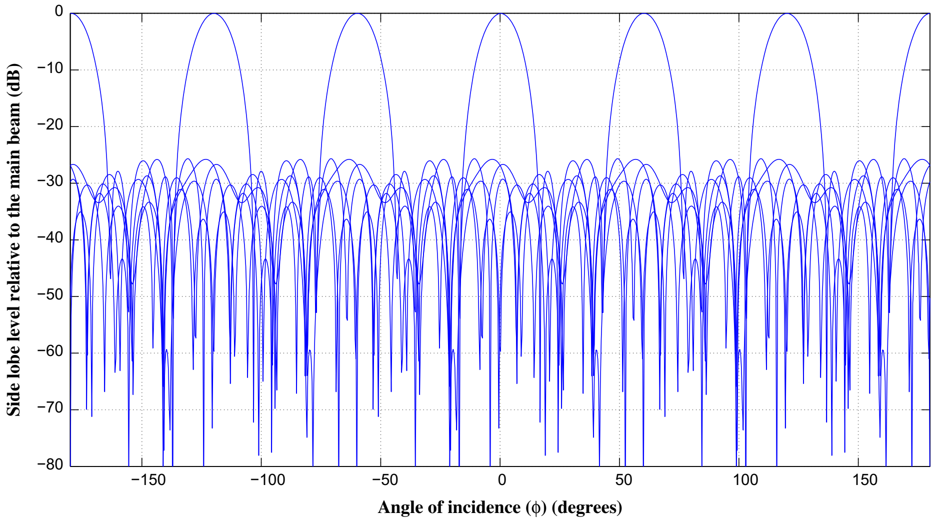

Figure 5. Array factor generated by the designed solution ($SLL = -25.66$ dB and $DIR = 15.36$ dB).

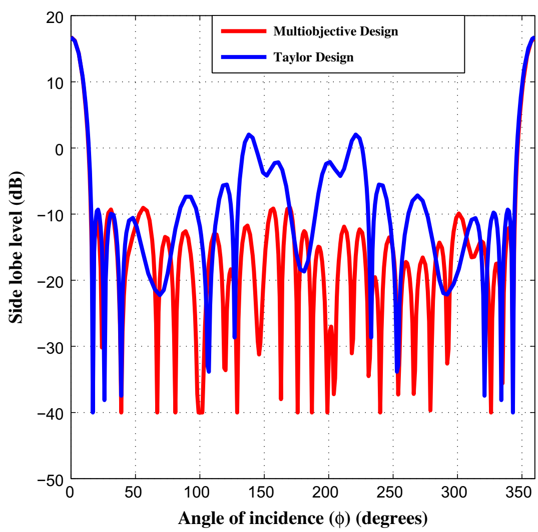

Figure 6. Comparison between the array factor generated by the multi-objective design solution and the Taylor method.

better performance than a concentric rings antenna array with the optimization of the amplitude values only.

When obtaining multiple Pareto solutions the decision-maker, i.e. the antenna designer, needs to specify a posteriori choice criterion that helps to select a single solution. In this case, the criterion will usually consider the following aspect: the two criteria, i.e. the side lobe level and the directivity, can be weighted in accordance with the designer's specific design goal. For instance, some applications may require a given directivity and the lowest possible side lobe level. As a design example, consider the case of lowest side lobe level obtained in Figure 3 ($SLL = -25.66$ dB and

DIR = 15.36 dB). The array factor generated by this design solution is illustrated in Figure 5. As shown in Figure 5, the optimization of the array can maintain a low side lobe level and directivity without pattern distortion during beam steering.

Finally, Figure 6 illustrates a comparison between the array factor generated by the multi-objective design solution (shown in Figure 5) and the array factor generated by the Taylor method.[7,31] As illustrated in Figure 6, the design case obtained by using multi-objective optimization presents a significant improvement in terms of the side lobe level (around 10 dB) considering the same directivity in both the cases. The method of Taylor provides an array factor considering the optimization of the amplitude values and a progressive phase excitation for beam-scanning. The evolutionary optimization allows us to deal with models of any degree of freedom in the multi-objective design case. Therefore, the multi-objective design solution provides an array factor considering the optimization of the values of amplitude and phase.

5. Conclusions

This paper illustrated the multi-objective design of concentric rings antenna arrays. In this design problem, a performance comparison to four evolutionary optimization algorithms was achieved. The obtained results illustrate that the methods of DEMO/parent and DEMO/closest/dec present a better performance in the trade-off curve computation in terms of the side lobe level and the directivity with respect to NSGA-II and EM-MOPSO under equal computation time. For the Set Coverage DEMO/closest/dec, a better performance with respect to DEMO/parent is presented. However, for the performance metric of the binary epsilon indicator DEMO/parent presented a better approximation to the Pareto front with respect to DEMO/closest/dec.

Furthermore, the results illustrated that the optimization of the array could provide low side lobe levels and high values of the directivity. This performance of the array is achieved without pattern distortion during beam steering in the whole azimuth plane (360°).

Acknowledgments

This work was supported by the Mexican National Science and Technology Council, CONACyT, under grant 127919 and the Science and Technology Council of Tamaulipas Mexico (COTACyT) under Grant TAMPS-2011-C35-185932.

References

[1] Panduro MA, Brizuela C. Evolutionary multi-objective design of non-uniform circular phased arrays. Internat. J. Comput. Math. Electrical and Electronic Eng. COMPEL. 2008;27:549–564. doi: 10.1108/03321640810847823. ISSN: 0332–1649.

[2] Zhang L, Jiao Y-C, Chen B, Weng Z-B. Multiobjective optimization design of concentric ring arrays with 3D beam scanning using differential evolution algorithm. Internat. J. Numerical Modell. 2012. doi: 10.1002/jnm.1864.

[3] Panduro MA, Covarrubias DH, Brizuela CA, Marante FR. A multi-objective approach in the linear antenna array design. AEU Internat. J. Elect. Commun. 2005;59:205–212.

[4] Panduro MA, Brizuela C, Covarrubias D. Design of electronically steerable linear arrays with evolutionary algorithms. Appl. Soft Comput. J. 2008;8:46-54. doi:10.1016/j.asoc.2006.10.011. ISSN:1568-4946.

[5] Robic T, Filipic B. DEMO: Differential evolution for multiobjective optimization. Lecture Notes Comp. Sci. 2005;3410:520–533.

[6] Coello C, Lechuga MS. MOPSO: a proposal for multiple objective particle swarm optimization. In: Proceedings of the 2002 Congress on Evolutionary Computation, CEC'02; 2002; Honolulu, HI. p. 1051–1056.

[7] Balanis C. Antenna theory-analysis and design. 3rd ed. New York: Wiley; 2005.
[8] Panduro MA, Brizuela CA, Balderas LI, Acosta D. A comparison of genetic algorithms, particle swarm optimization and the differential evolution method for the design of scannable circular antenna arrays. Progr. Electro. Re. B. 2009;13:171–186.
[9] Watanabe F, Goto N, Nagayama A, Yoshida G. A pattern synthesis of circular arrays by phase adjustment. IEEE Trans. Antennas Propag. 1980;28:857–863.
[10] Vescovo R. Constrained and unconstrained synthesis of array factor for circular arrays. IEEE Trans. Antennas Propag. 1995;43:1405–1410.
[11] Zhang S, Gong SX, Zhang PF. A modified PSO for low sidelobe concentric ring arrays synthesis with multiple constraints. J. Electromagn. Waves Appl. 2009;23:1535–1544.
[12] Dessouky M, Sharshar H, Albagory Y. A novel tapered beamforming window for uniform concentric circular arrays. J. Electromagn. Waves Appl. 2006;20:2077–2089.
[13] Chen TB, Dong YL, Jiao YC, Zhang FS. Synthesis of circular antenna array using crossed particle swarm optimization algorithm. J. Electromagn. Waves Appl. 2006;20:1785–1795.
[14] Li Y, Ho KC, Kwan C. 3-D array pattern synthesis with frequency invariant property for concentric ring. IEEE Trans. Signal Process. 2006;54:780–784.
[15] Haupt RL. Optimized element spacing for low sidelobe concentric ring arrays. IEEE Trans. Antennas Propag. 2008;56:266–268.
[16] Li F, Jiao Y-C, Ren L-S, Chen Y-Y, Zhang L. Pattern synthesis of concentric ring array antennas by differential evolution algorithm. J. Electromagn. Waves Appl. 2011;25:421–430.
[17] Zhang L, Jiao Y-C, Chen B. Optimization of concentric ring array geometry for 3D beam scanning. Int. J. Antennas Propagat. 2012;5. doi:10.1155/2012/625437.
[18] Zhang L, Jiao Y-C, Chen B, Weng Z-B. Design of wideband concentric-ring arrays with three-dimensional scanning based on the optimization of array geometry. Electromagnetics. 2012;32:305–320.
[19] Reyna A, Panduro MA, Covarrubias DH, Mendez A. Design of steerable concentric rings array for low side lobe level. Int. J. Sci. Technol. (Scientia Iranica) Trans. D: Electr. Eng. 2012;19:727–732.
[20] Deb K, Agrawal S, Pratap A, Meyarivan T. A fast elitist non-dominated sorting algorithm for multi-objective optimization: NSGA-II, parallel problem solving from nature – PPSN VI. Berlin: Springer; 2000. p. 849–858.
[21] Rahmat-Samii Y, Michielssen E. Electromagnetic optimization by genetic algorithms. New York: Wiley & Sons; 1999.
[22] Storn R, Price K. Minimizing the real functions of the ICEC'96 contest by differential evolution. Proceedings of the IEEE Conference, Evolutionary Computation; 1996; Nagoya.
[23] Thomsen R. Multimodal optimization using crowding-based differential evolution. In: 2004 Congress on Evolutionary Computation (CEC'2004). Volume 1; 2004; IEEE Service Center, Portland, Oregon, USA. p. 1382–1389.
[24] Kennedy J, Eberhart RC. Swarm intelligence. San Francisco (CA): Morgan Kaufmann; 2001.
[25] Janga Reddy M, Najesh Kumar D. An efficient multiobjective optimization algorithm based on swarm intelligence for engineering design. Eng. Optim. 2007;39:49–68.
[26] Eberhart RC, Shi, Y. Particle swarm optimization: Developments, applications and resources. In: Proceedings Congress, Evolutionary Computation; 2001; Seoul. p. 81–86.
[27] Eberhart R, Shi Y. Particle swarm optimization: developments, applications and resources. Proc. Cong. Evol. Comput. 2001;1:81–86.
[28] Jin N, Rahmat-Samii Y. Advances in particle swarm optimization for antenna designs: real-number, binary, single-objective and multiobjective implementations. IEEE Trans. Antennas Propag. 2007;55:556–567.
[29] Eberhart R, Shi Y. Evolving artificial neural networks. In Proc. Int. Conf. Neural Networks and, Brain; 1998. p. PL5–PL13.
[30] Zitzler E, Laumanns TM, Fonseca C, da Fonseca V. Performance assessment of multiobjective optimizers: An analysis and review. IEEE Trans. Evol. Comput. 2003;7:529–533.
[31] Commercially available Antenna Magus software. Available from: www.antennamagus.com